

On the kinetics of high intensity illuminated annealing of n-type SHJ solar cells: 0.4%_{abs} efficiency gain in one second

Matthew Wright^{a,*}, Anastasia H. Soeriyadi^b, Moonyong Kim^b, Brendan Wright^b,
Bruno Vicari Stefani^c, Dmitry Andronikov^{d,e}, Ilia Nyapshaev^{d,e}, Sergey Abolmasov^{d,e},
Alexey Abramov^{d,e}, Ruy S. Bonilla^a, Brett Hallam^b

^a Department of Materials, University of Oxford, Oxford, OX1 3PH, United Kingdom

^b School of Photovoltaics and Renewable Energy Engineering (SPREE), The University of New South Wales (UNSW), Sydney, 2052, Australia

^c CSIRO Energy, Newcastle Energy Centre, 10 Murray Dwyer Circuit, Mayfield West, NSW, 2304, Australia

^d R&D Center of Thin Film Technologies in Energetics Hevel Solar, St. Petersburg, 194064, Russia

^e Ioffe Institute, Russian Academy of Sciences, St. Petersburg, 194021, Russia

ARTICLE INFO

Keywords:

Silicon heterojunction solar cell
Light soaking
Kinetics
Illuminated annealing

ABSTRACT

Silicon heterojunction (SHJ) solar cells are at the forefront of high efficiency industrial solar cell manufacturing. The rapid increase in efficiency compared with passivated emitter and rear cell (PERC) cells has significantly propelled commercial interest in this technology. Illuminated annealing under elevated temperatures has been shown to lead to efficiency enhancements in SHJ cells. Recently, it was observed that increasing the light intensity used during the annealing can accelerate the efficiency gains, this approach has started to be incorporated into SHJ manufacturing. In this work, we investigate the kinetics of this high intensity illuminated annealing process in the temperature range from 200 °C to 300 °C, demonstrating that the kinetics and extent of the efficiency gain strongly depend on the temperature of the process. For the first time, we show that the changes in V_{OC} and R_S , which control the efficiency enhancement, occur at different rates. Remarkably, by investigating the temperature dependence we demonstrate a process that leads to efficiency gains of >0.4%_{abs} in only 1 s. This new understanding presents a pathway to an industrially compatible annealing approach that significantly increases the power output of SHJ modules.

1. Introduction

Silicon heterojunction (SHJ) solar cells have attracted increasing commercial interest over the past few years [1,2]. In 2017, the world record efficiency for a single junction silicon solar cell of 26.7% was achieved using this approach [3]. Since this achievement, many companies have turned their attention to this technology, due to the promise for high efficiency single junction cells and the compatibility with tandem architectures [4,5]. LONGi solar recently demonstrated a SHJ solar cell fabricated in an industrial environment with efficiency exceeding 26% [6]. The performance of various silicon solar cell architectures in the presence of illumination (or carrier generation via current injection) and elevated temperature has been the subject of intense study for decades [7–13]. In p-type solar cells doped with boron, illumination was shown to cause bulk degradation, attributed to the formation of recombination-active boron-oxygen complexes [7,14]. More recently,

illumination under elevated temperature conditions was shown to cause another form of bulk degradation in many types of silicon, referred to as light and elevated temperature degradation (LeTID) [15,16]. As the kinetics of such bulk degradation modes are dependent on the illumination intensity, high intensity illumination with a laser is one approach to accelerate the degradation and recovery of boron oxygen light-induced degradation (BO LID) [14,17,18] and LeTID [19]. Such accelerated processes have also led to efficiency enhancements in both passivated emitter and rear cell (PERC) [20] and tunnel oxide passivated contact (TOPCon) [21] solar cells.

The operation of SHJ solar cells is largely governed by the interactions at the hydrogenated amorphous silicon (a-Si:H)/crystalline silicon (c-Si) interface [22]. The excellent surface passivation achieved at this interface is one of the reasons that SHJ cells have exhibited such high open-circuit voltage (V_{OC}) [22,23]. Exposure to extended light soaking has been reported to cause efficiency enhancements for SHJ

* Corresponding author.

E-mail address: matthew.wright@materials.ox.ac.uk (M. Wright).

<https://doi.org/10.1016/j.solmat.2022.112039>

Received 30 April 2022; Received in revised form 16 September 2022; Accepted 1 October 2022

Available online 11 October 2022

0927-0248/© 2022 The Authors. Published by Elsevier B.V. This is an open access article under the CC BY license (<http://creativecommons.org/licenses/by/4.0/>).

solar cells [12,24,25]. Kobayashi et al. demonstrated an efficiency enhancement of 0.3%_{abs} after light soaking n-type SHJ cells under 1 sun light soaking conditions [26]. This enhancement was correlated with improvements in chemical passivation at the a-Si:H/c-Si interface, and was shown to be most pronounced in samples that had a higher concentration of initial interface defect states [27]. In our previous work, we have showed that replacing the 1 sun illumination source with a high intensity laser can both significantly accelerate and increase the magnitude of the efficiency enhancement. Such a process can lead to an efficiency enhancement of 0.7%_{abs} [28–30]. Bao et al. also demonstrated efficiency enhancements in n-type SHJ under laser illumination [31]. Several leading SHJ manufacturers have incorporated similar processes into production over the past 12 months. In this work, we provide a comprehensive analysis of the kinetics of this accelerated process. We detail the influence of temperature on the changes in efficiency and demonstrate it is possible to increase the efficiency by >0.4%_{abs} with a 1 s process.

2. Results and discussion

The impact of illuminated annealing at various temperatures on the efficiency of n-type SHJ cells is shown in Fig. 1 (a). For all annealing temperatures, the efficiency increases during the time scale of the experiment. From this plot, we can see that the rate of efficiency increase depends on the temperature. For the lowest temperature, 205 °C, the efficiency rises slowly, reaching a peak after 100 s, followed by a gradual reduction in efficiency. At this temperature, a maximum efficiency increase of 0.60%_{abs} is observed. For the highest temperature investigated, 295 °C, the efficiency increases much more rapidly and begins to reduce after only 3 s. Previous reports investigating the impact of light soaking under 1 sun illumination have indicated that the efficiency enhancement is related to both increased V_{OC} and FF [26,30,32]. Fig. 1 (b) displays the impact of illuminated annealing on V_{OC} . The impact of temperature on the kinetics of change in V_{OC} is clear, the V_{OC} rises more quickly when the temperature of the process is increased. Multiple prior reports have attributed the increased V_{OC} to a reduction in the concentration of interface defect states [26,27]. This was also observed by Kobayashi

et al. when light soaking was replaced by direct current injection, indicating that the enhancement is facilitated by carrier generation in c-Si [26]. Fig. 1 (c) displays the change in FF. Again, the FF increases for all temperatures and the increase is dependent on the temperature, however, as the spread of initial values is on the order of 1%_{abs}, it is difficult to directly infer the temperature dependence. In addition to changes in the V_{OC} and FF, the kinetics of J_{SC} for all temperatures is shown in Fig. 1 (d). In the time frame investigated in this experiment, the J_{SC} for the 205 °C case does not display a significant change. However, interestingly, for all other temperatures, a reduction in J_{SC} does occur, this occurs at shorter time frames as the temperature is increased. A reduction of up to 0.28 mA/cm² is seen for the 295 °C case, which has an impact on the efficiency. Reduced J_{SC} was not observed in our previous results of illuminated annealing on n-type SHJ cells made at Hevel LLC [30]. Previous reports indicated that J_{SC} was consistent before/after the process, however, importantly, only one condition was used in our previous study, 255 °C for 30 s. The corresponding data point in Fig. 1(d) shows a reduction of only 0.06 mA/cm².

As shown in Fig. 1 (a), the average initial efficiency of each group varies by $\sim 0.20\%$ _{abs}. As the magnitude of efficiency enhancement induced by illuminated annealing is between 0.40%_{abs} to 0.60%_{abs}, this variance in the starting efficiency makes it difficult to compare. Fig. 2 (a) displays the normalized change in average efficiency, to more clearly depict the changes. When assessing the efficiency change after 1 s of processing, a clear trend is observed. Increasing the temperature leads to a more rapid efficiency increase. Remarkably, for the highest temperature of 295 °C, an average efficiency gain of 0.41%_{abs} was achieved with only 1 s of processing. The amount of time required to reach the maximum gain in efficiency was extracted from this graph and plotted as a function of the processing temperature in Fig. 2 (b). The linear fit to this data is very accurate, with $R^2 = 0.9942$. Multiple reports have indicated that this efficiency enhancement is caused by more than one change occurring in the cell [25,26,30]. Kobayashi et al. correlated the increased V_{OC} with decreased density of interfacial surface states, leading to improved surface passivation [26]. We have previously shown that 80% of the change in FF following illuminated annealing is related to a reduction in series resistance (R_s), while the remaining

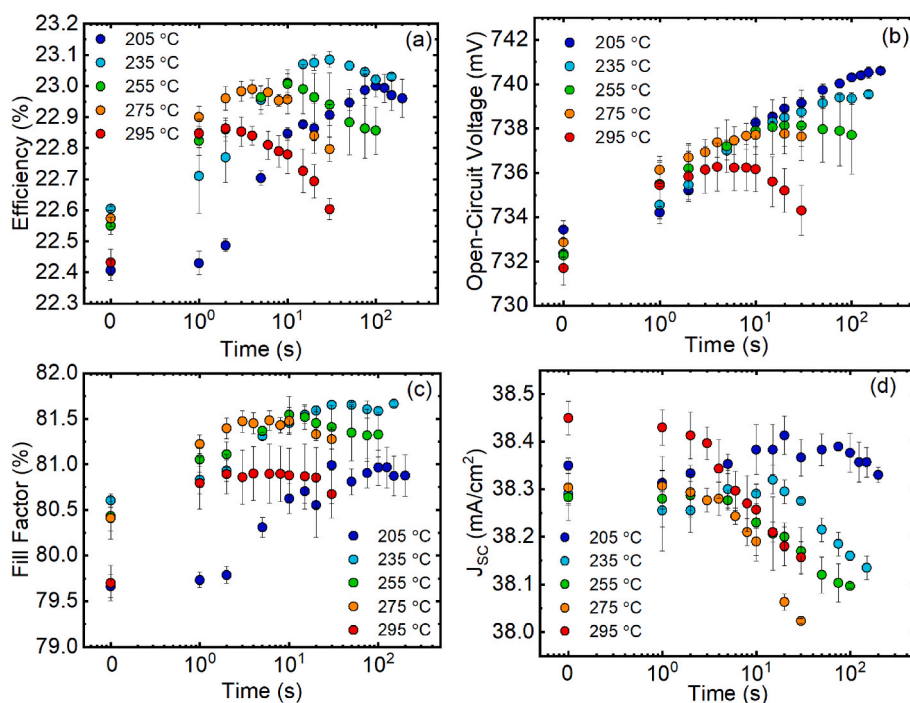


Fig. 1. The impact of illuminated annealing on (a) efficiency, (b) V_{OC} , (c) FF and (d) J_{SC} . Three identical cells were measured for each condition, the error bars represent the standard deviation.

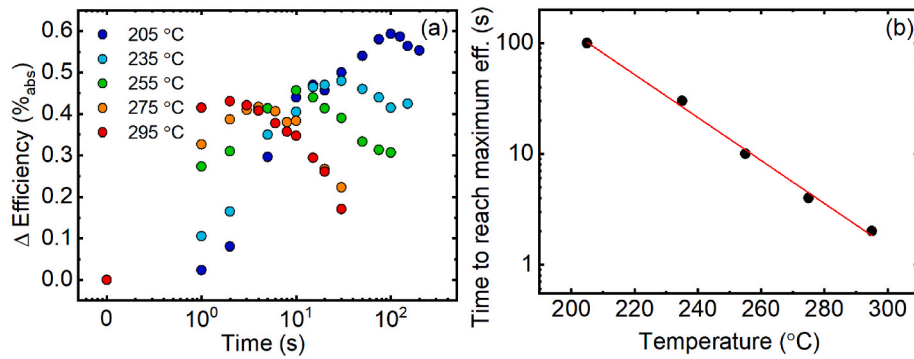


Fig. 2. (a) Normalized change in absolute efficiency as a function of illuminated annealing time. For each temperature, the value is normalized to the average efficiency for the three cells in that group. (b) Time taken to reach the maximum efficiency enhancement, plotted as a function of the actual sample temperature.

change is seen in the pseudo fill factor (pFF) [30]. As the efficiency data shown in Fig. 2 (a) is a combination of competing effects, the changes in both V_{OC} and R_S are normalized and plotted in Fig. 3.

Fig. 3 (a) shows the normalized change in V_{OC} for the different temperatures. It is clear that increasing the temperature increases the rate at which V_{OC} increases. The thermal activation of the V_{OC} increase was investigated using the Arrhenius formalism. The change in V_{OC} for each temperature was modelled using a stretched exponential function. From the model, the rate of change in V_{OC} ($k_{\Delta V_{OC}}$) was extracted and plotted as a function of inverse temperature. This is shown in Fig. 3 (b). The Arrhenius relation for thermal activation in equation (1) was then used to extract the activation energy (E_A) of the process by analysing the slope in Fig. 3 (b). This resulted in an E_A of 0.17 eV.

$$k(T) = k_0 \exp\left(\frac{-E_A}{kT}\right) \quad (1)$$

The normalized change in R_S is shown in Fig. 3 (c). The same formalism was applied to this data to compare the thermal activation of V_{OC} and R_S ; however, it was not possible to accurately fit the R_S reaction rates with an Arrhenius relationship. Observation of the data also suggests that the change in R_S does not follow a direct relationship with the temperature of the process, unlike for V_{OC} . Additionally, by comparing the changes in Fig. 3 (a) and Fig. 3 (c) after 1 s of illuminated annealing, it is apparent that the changes in R_S occur much more rapidly than the increase in V_{OC} .

To better visualise the differences in the rates of V_{OC} increase and R_S reduction, PL images and R_S mapping was used. Fig. 4 (a) displays 1 sun open-circuit PL images of a cell processed at 255 °C for 0 s, 2 s and 30 s. Changes in the PL counts are representative of changes in the V_{OC} [33]. After 2 s, the PL counts are only slightly increased. Following 30 s of illuminated annealing, the counts are still slowly rising. These images closely correlate with the changes in V_{OC} represented in Fig. 3 (a). Fig. 4 (b) display R_S maps of an identical cell that underwent the same processing. In contrast to the PL image, Fig. 4 (e) shows that 2 s of processing causes a rapid reduction in R_S . Over the subsequent 30 s of processing, however, the R_S is observed to be quite stable. This provides a visual representation of the observed difference in the rates of change for both V_{OC} and R_S .

3. Discussion

We first turn our attention to the changes in V_{OC} . For this case, there appears to be a clear thermal activation and the rate of change is notably slower than for R_S . The current hypothesis for the improved surface passivation following light soaking (in the presence of doped a-Si:H layers) involves four steps, i) the generation of carriers in the c-Si, which leads to recombination near the c-Si/a-Si:H(i) interface, ii) a weakening of hydrogen ions bonding in the a-Si:H(i) induced by this trapped charge, iii) the migration of hydrogen ions to the interface in the

presence of the doped a-Si:H layer, iv) hydrogen bonding with surface interface states, causing a reduction in surface recombination [24,34]. This hypothesis is supported by observations from Mahtani et al. who showed a reduction in the rate of surface passivation improvement for thicker a-Si:H(i) films [27]. As such, this improved surface passivation is seemingly dependent on the rate of diffusion of hydrogen through the a-Si:H(i). It is well known that this rate of diffusion is both slow (relative to the movement of hydrogen in c-Si) and follows a clearly defined temperature dependence [35,36]. This may explain the relatively slow, temperature dependent changes in V_{OC} observed in Fig. 3(a).

In contrast, the reduction in R_S induced by light soaking effects is less well understood. Veirman et al. recently provided a tentative explanation for this observation by the fabrication of SHJ TLM samples that isolated the current path [37]. They showed that following light soaking the sheet resistance of the front ITO layer reduced from 190 Ω/sq to 175 Ω/sq . A similar observation of improved conductivity in the ITO following light soaking was presented by Pingel et al. [38]. In this case, it appears that the mechanism governing reductions in R_S may be completely different in nature to the increases in V_{OC} , which could explain the vastly different changes observed under illuminated annealing. In this work, all samples were processed under illumination. The reason for this is that high intensity light is required to maximise the efficiency gains in SHJ cells. Madumelu et al. compared 1 sun illumination and dark annealing at 160 °C. They showed that a similar reduction in R_S was observed under illumination and in the dark. This may indicate that the changes in R_S , which are tentatively attributed to increased conductivity in the ITO, are driven by a thermal process, rather than illumination. More work is required to better understand the changes in R_S .

The mechanism causing the increased V_{OC} is related to the generation of carriers in the c-Si, rather than simply the exposure to light. This raises the question of whether it would be possible to replace the high intensity light source with a direct injection of carriers. Several reports have demonstrated efficiency enhancements via a forward electric bias treatment in the dark, with an applied forward current density with equivalent carrier generation to 1 sun illumination [24,26]. The generation of carriers is also required for the stabilisation of degradation modes in p-type cells such as PERC. In an industrial setting, carrier injection can be a favourable method to achieve this, compared to light soaking. In this case, cells are stacked together in a 'coin stacking' arrangement and a forward bias is applied. Typically, the forward current density generates a density of minority carriers comparable to that of 1 sun illumination conditions. However, the main advantage of the results presented in this paper is that the high intensity laser is able to generate carrier densities that are much higher than 1 sun illumination conditions. As such, we believe that an equivalent forward electric bias treatment is not as suitable for the treatment of SHJ solar cells. This is related to three main factors: i) to generate an equivalent density of carriers, the applied forward current density would have to be very

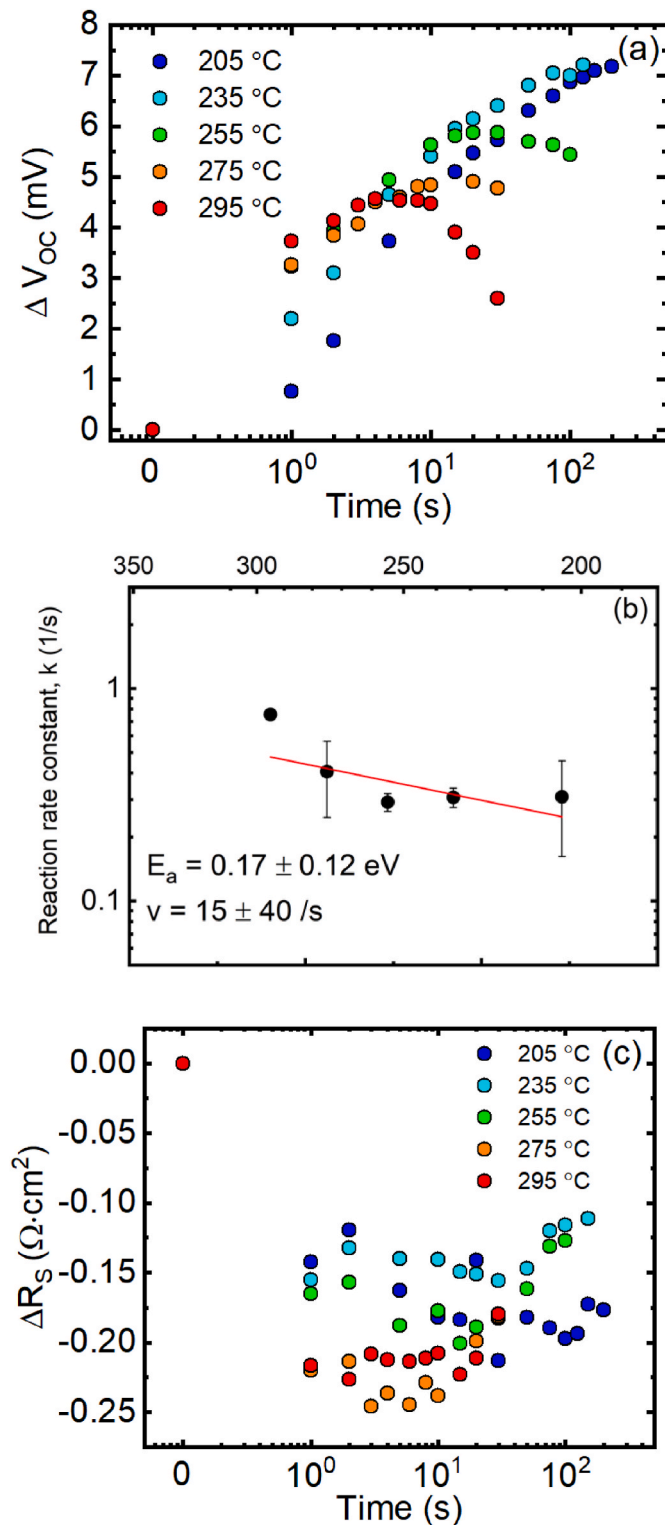


Fig. 3. (a) Change in normalized V_{OC} , (b) Arrhenius plot displaying the rate of ΔV_{OC} as a function of inverse temperature, (c) change in normalized R_S .

large, which would likely damage the contacts, ii) the thickness of SHJ cells is reducing and the surfaces are very sensitive to defects. As such, the physical handling required for coin stacking could cause serious yield issues. iii) If a carrier injection comparable to 1 sun illumination was employed to avoid damaging the contacts, the timescale of the treatment would be too slow.

It is well known that the SHJ cell approach is a low temperature route

for fabricating industrial silicon solar cells. However, the precise upper limit on the processing temperature is not clear. The processes that require such elevated temperatures include the deposition of the a-Si films and any other subsequent annealing process. During the growth of the a-Si:H(i) films, it is important to limit the temperature such that epitaxial growth of the layers is avoided. De Wolf et al. showed that epitaxial growth of the intrinsic layer can occur for deposition temperatures exceeding 200 °C [39]. A following process is also required for curing the low-temperature metal paste and healing sputter damage. De Wolf et al. showed that for surface passivation in the presence of a doped a-Si overlayer, as is present in a cell, the surface passivation may deteriorate for subsequent annealing temperatures of >220 °C [23]. They postulate that the presence of the doped layer reduces the Si–H rupture bond rupture energies at the c-Si/a-Si:H(i) interface, thus, the deterioration in surface passivation was attributed to an effusion of H_2 from the interface at moderate temperature. However, the change in surface passivation following annealing is heavily dependent on the deposition temperature of the passivating layers, thus complicating the optimum thermal budget [39]. In fact, Shi et al. showed that a hydrogen plasma treatment performed at 450 °C could restore the lifetime of SHJ precursor samples that had deteriorated passivation due to annealing treatments, indicating that the deterioration of surface passivation is related to a loss of hydrogen from the interface [40]. In commercial production, the processing conditions for SHJ cells are typically <230 °C. In this study, we show that with a high-temperature illuminated annealing process, SHJ cells can tolerate temperatures up to 70 °C above this. In fact, this can be beneficial to cell performance. One very important distinction to make between the results presented here and previous annealing studies by De Wolf et al. [23,39] is the time of the process. In their studies, De Wolf et al. perform annealing for 30 min at each temperature. Due to the acceleration of surface kinetics induced by the very high intensity illumination used in this study, we are able to observe large changes in a matter of seconds. This may imply that a rethinking of the thermal budget for SHJ processing is required, if the passivation enhancements can be rapidly accelerated by carrier generation, the upper limit on temperature before degradation occurs may be increased.

4. Conclusion

Here, we study the kinetics of illuminated annealing of SHJ cells under high intensity light from a laser, with an illumination intensity equivalent to 100 suns. We show that the efficiency enhancement is governed by two processes: an increase in V_{OC} , likely linked to improved surface passivation, and a reduction in R_S . We additionally show that these two processes occur at different rates. The R_S reduction occurs much more quickly than the improvements in surface passivation that causes increased V_{OC} and it is less dependent on temperature. By modulating the temperature of the process, an efficiency enhancement of >0.4%_{abs} was achieved within a 1 s time frame. These results contradict the typical processing paradigm, which dictates that industrial SHJ cells are processed at < 230 °C. If applied to a 400 W module consisting of 24% efficiency SHJ cells, this process could increase the power output by 10 W.

5. Experimental section/methods

Experiments were performed on n-type silicon heterojunction cells, fabricated in an industrial environment by Hevel LLC. The cells were bifacial, 157.35 mm × 157.35 mm and had 5 busbars. The as-manufactured cells had an average efficiency of $22.50 \pm 0.08\%$. The high intensity illuminated annealing was performed at UNSW with a laser, a detailed overview of the experimental setup is described in Ref. [30]. During illumination, the samples were placed on a hotplate, a robotic arm was used to ensure that the time of the process was precisely controlled. Our previous study used a hotplate setpoint temperature of

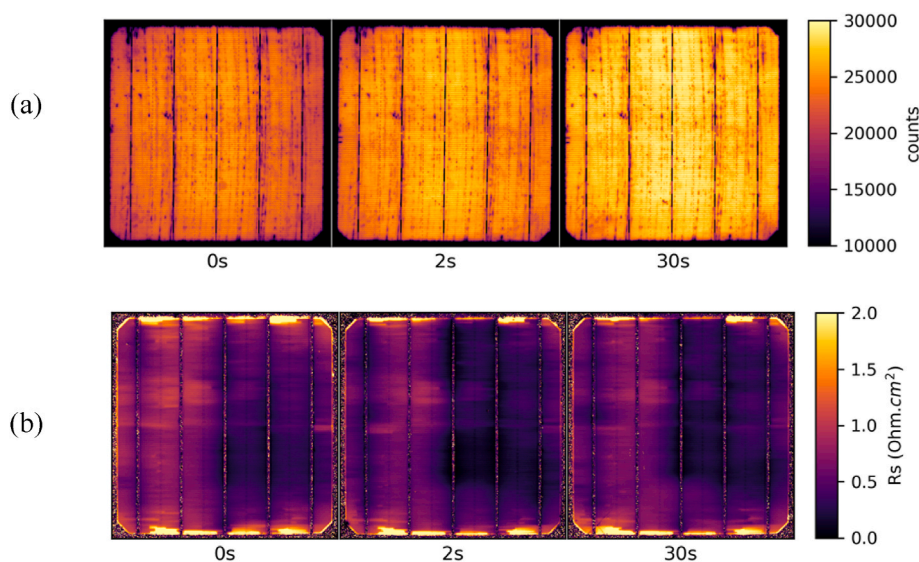


Fig. 4. (a) Photoluminescence images and (b) R_s mapping of n-type SHJ cells that underwent illuminated annealing at 255 °C for 0 s, 2 s and 30 s.

200 °C [30]. In this report, the hotplate setpoint temperature was varied from 150 °C to 250 °C. The illumination causes the sample temperature to increase during the process. As such, the actual temperature of the samples during the annealing is higher than the setpoint temperature. Table 1 indicates the relationship between the setpoint temperature of the hotplate and the corresponding actual sample temperature, measured using an IR gun after ~10 s of illumination. During the first few seconds of illumination, the temperature rapidly rises from the setpoint temperature to the stabilized temperature. Thus, the first few seconds of data will not be at exactly the stable temperature shown in Table 1.

One-sun I–V measurements were then taken using a pv tools Loana IV testing system under standard testing conditions. Three identical cells were measured for each condition, the error bars shown in Fig. 1 correspond to the standard deviation of the three cells. Photoluminescence (PL) images were taken using a BT imaging LIS-R3 luminescence imaging tool before and after the illuminated annealing. The same tool was used to generate the series resistance mapping, this analysis was based on the formalism developed by Kampwerth et al. [41].

Supporting Information

Details of the fitting procedure for Fig. 3(a), are included as Supporting Information and available free of charge at <https://www.journals.elsevier.com/solar-energy-materials-and-solar-cells>.

CRediT authorship contribution statement

Matthew Wright: Writing – review & editing, Writing – original draft, Methodology, Investigation, Conceptualization. **Anastasia H. Soeriyadi:** Writing – review & editing, Investigation, Formal analysis, Data curation. **Moonyong Kim:** Writing – review & editing, Software, Investigation, Formal analysis, Data curation. **Brendan Wright:** Writing – review & editing, Software, Methodology, Formal analysis, Data curation. **Bruno Vicari Stefani:** Writing – review & editing, Formal analysis, Data curation. **Dmitry Andronikov:** Writing – review & editing, Resources, Methodology, Investigation. **Ilia Nyapshaev:** Resources, Methodology, Investigation. **Sergey Abolmasov:** Resources, Methodology, Investigation. **Alexey Abramov:** Resources, Methodology, Investigation. **Ruy S. Bonilla:** Writing – review & editing, Supervision, Project administration, Funding acquisition. **Brett Hallam:** Writing – review & editing, Supervision, Project administration, Methodology,

Table 1

Hotplate setpoint temperature and the corresponding sample temperature, as measured using an IR gun.

Setpoint temperature (°C)	Sample temperature (°C)
150	205
175	235
200	255
225	275
250	295

Conceptualization.

Declaration of competing interest

The authors declare that they have no known competing financial interests or personal relationships that could have appeared to influence the work reported in this paper.

Data availability

All data created during this research and published in this article is openly available from the Oxford University Research Archive and can be downloaded free of charge from <http://ora.ox.ac.uk>.

Acknowledgements

This work was supported by the Australian Government through the Australian Center for Advanced Photovoltaics (ACAP) and the Australian Renewable Energy Agency (ARENA) (2017/RND005). The views expressed herein are not necessarily the views of the Australian Government, and the Australian Government does not accept responsibility for any information and advice contained herein. A.H.S and M.K. would like to acknowledge the support of ACAP for their fellowships. The authors thank Nino Borojevic, Zhen Yang and Fred Qi of the UNSW Solar Industrial Research Facility. All the authors are thankful to Radka Chakalova for assistance in clean-room processing. R.S.B was supported by the Royal Academy of Engineering under the Research Fellowship scheme. This work was supported by the UK Engineering and Physical Sciences Research Council grant number EP/V038605/1. For the purpose of Open Access, the author has applied a CC BY public copyright licence to any Author Accepted Manuscript (AAM) version arising from this submission.

References

- [1] S. De Wolf, A. Descoedres, Z.C. Holman, C. Ballif, High-efficiency silicon heterojunction solar cells: a review, *Greenpeace* 2 (2012) 7–24.
- [2] A.S. Abramov, D.A. Andronikov, S.N. Abolmasov, E.I. Terukov, Silicon heterojunction technology: a key to high efficiency solar cells at low cost, in: V. Petrova-Koch, R. Hezel, A. Goetzberger (Eds.), *High-Efficient Low-Cost Photovoltaics Recent Dev*, Springer International Publishing, Cham, 2020, pp. 113–132, https://doi.org/10.1007/978-3-030-22864-4_7.
- [3] K. Yoshikawa, H. Kawasaki, W. Yoshida, T. Irie, K. Konishi, K. Nakano, T. Uto, D. Adachi, M. Kanematsu, H. Uzu, K. Yamamoto, Silicon heterojunction solar cell with interdigitated back contacts for a photoconversion efficiency over 26, *Nat. Energy* 2 (2017), 17032, <https://doi.org/10.1038/nenergy.2017.32>.
- [4] Z. Yu, M. Leilaoui, Z. Holman, Selecting tandem partners for silicon solar cells, *Nat. Energy* 1 (2016), 16137.
- [5] J. Werner, B. Niesen, C. Ballif, Perovskite/silicon tandem solar cells: marriage of convenience or true love story? – an overview, *Adv. Mater. Interfac.* 5 (2018), 1700731, <https://doi.org/10.1002/admi.201700731>.
- [6] LONGi, https://en.longi-solar.com/home/events/press_detail/id/364.html.
- [7] H. Fischer, W. Pischner, Investigation of Photon and Thermal Induced Changes in Silicon Solar Cells, 10th IEEE PVSC, 1973, pp. 404–411.
- [8] J. Lindroos, H. Savin, Review of light-induced degradation in crystalline silicon solar cells, *Sol. Energy Mater. Sol. Cells* 147 (2016) 115–126, <https://doi.org/10.1016/j.solmat.2015.11.047>.
- [9] D. Chen, M. Vaquero Contreras, A. Ciesla, P. Hamer, B. Hallam, M. Abbott, C. Chan, Progress in the understanding of light- and elevated temperature-induced degradation in silicon solar cells: a review, *Prog. Photovoltaics Res. Appl.* n/a (2020), <https://doi.org/10.1002/pip.3362>.
- [10] D. Sperber, A. Herguth, G. Hahn, Instability of dielectric surface passivation quality at elevated temperature and illumination, *Energy Proc.* 92 (2016) 211–217, <https://doi.org/10.1016/j.egypro.2016.07.061>.
- [11] A. Herguth, G. Schubert, M. Käs, G. Hahn, M. Käs, G. Hahn, A new approach to prevent the negative impact of the metastable defect in boron doped Cz silicon solar cells, in: 4th IEEE World Conf. Photovolt. Energy Convers, 2006, pp. 940–943, <https://doi.org/10.1109/WCPEC.2006.279611>. IEEE.
- [12] J. Yu, P.S. Leonard, D. Qiu, Y. Zhao, A. Lambert, C. Zahren, L. Volker, W. Duan, J. Yu, K. Ding, Light-induced performance of SHJ solar modules under 2000 h illumination, *Sol. Energy Mater. Sol. Cells* 235 (2022), 111459, <https://doi.org/10.1016/j.solmat.2021.111459>.
- [13] S.W. Glunz, S. Rein, W. Warta, J. Knobloch, W. Wettling, Degradation of carrier lifetime in Cz silicon solar cells, *Sol. Energy Mater. Sol. Cells* 65 (2001) 219–229, [https://doi.org/10.1016/S0927-0248\(00\)00098-2](https://doi.org/10.1016/S0927-0248(00)00098-2).
- [14] B. Vicari Stefani, A. Soeriyadi, M. Wright, D. Chen, M. Kim, Y. Zhang, B. Hallam, Large-area boron-doped 1.6 Ω cm p-type Czochralski silicon heterojunction solar cells with a stable open-circuit voltage of 736 mV and efficiency of 22.0, *Sol. RRL* 4 (2020), <https://doi.org/10.1002/solr.202000134>, 2000134.
- [15] F. Kersten, P. Engelhart, H.-C. Ploigt, A. Stekolnikov, T. Lindner, F. Stenzel, M. Bartsch, A. Szpeth, K. Petter, J. Heitmann, J.W. Müller, Degradation of multicrystalline silicon solar cells and modules after illumination at elevated temperature, *Sol. Energy Mater. Sol. Cells* 142 (2015) 83–86, <https://doi.org/10.1016/j.solmat.2015.06.015>.
- [16] C. Sen, C. Chan, P. Hamer, M. Wright, C. Chong, B. Hallam, M. Abbott, Eliminating light- and elevated temperature-induced degradation in P-type PERC solar cells by a two-step thermal process, *Sol. Energy Mater. Sol. Cells* 209 (2020), 110470, <https://doi.org/10.1016/j.solmat.2020.110470>.
- [17] B.J. Hallam, A.M. Ciesla, C.C. Chan, A. Soeriyadi, S. Liu, A.M. Soufiani, M. Wright, S. Wenham, Overcoming the challenges of hydrogenation in silicon solar cells, *Aust. J. Chem.* 71 (2018) 743–752, <https://doi.org/10.1071/CH18271>.
- [18] P. Hamer, B. Hallam, M. Abbott, S. Wenham, Accelerated formation of the boron-oxygen complex in p-type Czochralski silicon, *Phys. Status Solidi Rapid Res. Lett.* 9 (2015) 297–300, <https://doi.org/10.1002/psr.201510064>.
- [19] D.N.R. Payne, C.E. Chan, B.J. Hallam, B. Hoex, M.D. Abbott, S.R. Wenham, D. M. Bagnall, Acceleration and mitigation of carrier-induced degradation in p-type multi-crystalline silicon, *Phys. Status Solidi Rapid Res. Lett.* 10 (2016) 237–241, <https://doi.org/10.1002/psr.201510437>.
- [20] R. Chen, H. Tong, H. Zhu, C. Ding, H. Li, D. Chen, B. Hallam, C.M. Chong, S. Wenham, A. Ciesla, 23.83% efficient mono-PERC incorporating advanced hydrogenation, *Prog. Photovoltaics Res. Appl.* n/a (2020), <https://doi.org/10.1002/pip.3243>.
- [21] R. Chen, M. Wright, D. Chen, J. Yang, P. Zheng, X. Zhang, S. Wenham, A. Ciesla, 24.58% efficient commercial n-type silicon solar cells with hydrogenation, *Prog. Photovoltaics Res. Appl.* 29 (2021) 1213–1218, <https://doi.org/10.1002/pip.3464>.
- [22] R.V.K. Chavali, S. De Wolf, M.A. Alam, Device physics underlying silicon heterojunction and passivating-contact solar cells: a topical review, *Prog. Photovoltaics Res. Appl.* 26 (2018) 241–260, <https://doi.org/10.1002/pip.2959>.
- [23] S. De Wolf, M. Kondo, Boron-doped a-Si:H/c-Si interface passivation: degradation mechanism, *Appl. Phys. Lett.* 91 (2007), 112109, <https://doi.org/10.1063/1.2783972>.
- [24] J. Cattin, D. Petri, J. Geissbühler, M. Despeisse, C. Ballif, M. Boccard, Transferability of the light-soaking benefits on silicon heterojunction cells to module, *IEEE J. Photovoltaics* (2022) 1–7, <https://doi.org/10.1109/JPHOTOV.2021.3113861>.
- [25] J. Cattin, L.-L. Senaud, J. Haschke, B. Paviet-Salomon, M. Despeisse, C. Ballif, M. Boccard, Influence of light soaking on silicon heterojunction solar cells with various architectures, *IEEE J. Photovoltaics* 11 (2021) 575–583, <https://doi.org/10.1109/JPHOTOV.2021.3065537>.
- [26] E. Kobayashi, S. De Wolf, J. Levrat, G. Christmann, A. Descoedres, S. Nicolay, M. Despeisse, Y. Watabe, C. Ballif, Light-induced performance increase of silicon heterojunction solar cells, *Appl. Phys. Lett.* 109 (2016), 153503, <https://doi.org/10.1063/1.4964835>.
- [27] P. Mahtani, R. Varache, B. Jovet, C. Longeaud, J.-P. Kleider, N.P. Kherani, Light induced changes in the amorphous–crystalline silicon heterointerface, *J. Appl. Phys.* 114 (2013), 124503, <https://doi.org/10.1063/1.4821235>.
- [28] M. Wright, M. Kim, P. Dexiang, X. Xin, Z. Wenbin, B. Wright, B. Hallam, Multifunctional process to improve surface passivation and carrier transport in industrial n-type silicon heterojunction solar cells by 0.7% absolute, *AIP Conf. Proc.* 2147 (2019), 110006, <https://doi.org/10.1063/1.5123882>.
- [29] M. Wright, B.V. Stefani, A. Soeriyadi, R. Basnet, C. Sun, W. Weigand, Z. Yu, Z. Holman, D. Macdonald, B. Hallam, Progress with defect engineering in silicon heterojunction solar cells, *Phys. Status Solidi Rapid Res. Lett.* 15 (2021), 2100170, <https://doi.org/10.1002/psr.202100170>.
- [30] M. Wright, A. Soeriyadi, B. Wright, D. Andronikov, I. Nyaphaev, S. Abolmasov, A. Abramov, B. Hallam, High-intensity illuminated annealing of industrial SHJ solar cells: a pilot study, *IEEE J. Photovoltaics* 12 (2021) 267–273, <https://doi.org/10.1109/JPHOTOV.2021.3122932>.
- [31] S. Bao, L. Yang, J. Huang, Y. Bai, J. Yang, J. Wang, L. Lu, L. Feng, X. Bai, F. Ren, D. Li, H. Jia, The rapidly reversible processes of activation and deactivation in amorphous silicon heterojunction solar cell under extensive light soaking, *J. Mater. Sci. Mater. Electron.* (2021), <https://doi.org/10.1007/s10854-020-05146-0>.
- [32] E. Kobayashi, S. De Wolf, J. Levrat, A. Descoedres, M. Despeisse, F.-J. Haug, C. Ballif, Increasing the efficiency of silicon heterojunction solar cells and modules by light soaking, *Sol. Energy Mater. Sol. Cells* 173 (2017) 43–49, <https://doi.org/10.1016/j.solmat.2017.06.023>.
- [33] B. Hallam, B. Tjahjono, T. Trupke, S. Wenham, Photoluminescence imaging for determining the spatially resolved implied open circuit voltage of silicon solar cells, *J. Appl. Phys.* 115 (2014), 44901, <https://doi.org/10.1063/1.4862957>.
- [34] M. Stutzmann, W.B. Jackson, C.C. Tsai, Light-induced metastable defects in hydrogenated amorphous silicon: a systematic study, *Phys. Rev. B* 32 (1985) 23–47, <https://doi.org/10.1103/PhysRevB.32.23>.
- [35] J. Kakaliotis, R.A. Street, W.B. Jackson, Stretched-exponential relaxation arising from dispersive diffusion of hydrogen in amorphous silicon, *Phys. Rev. Lett.* 59 (1987) 1037.
- [36] H. Branz, Hydrogen diffusion and mobile hydrogen in amorphous silicon, *Phys. Rev. B* 60 (1999) 7725–7727.
- [37] J. Veirman, A. Leoga, L. Basset, W. Favre, O. Bonino, A. Le Priol, N. Rochat, D. Rouchon, Understanding the improvement of silicon heterojunction solar cells under light soaking, in: *AIP Conference Proceedings* 2487, 2021, p. 020017.
- [38] S. Pingel, Understanding the improvement of silicon heterojunction solar cells under light soaking, in: *12th Int. Conf. Cryst. Silicon Photovoltaics - Oral Presentation*, 2022.
- [39] S. De Wolf, H. Fujiwara, M. Kondo, Impact of annealing on passivation of a-Si:H/c-Si heterostructures, *Conf. Rec. IEEE Photovolt. Spec. Conf.* (2008) 1–4, <https://doi.org/10.1109/PVSC.2008.4922851>.
- [40] J. Shi, M. Boccard, Z. Holman, Plasma-initiated rehydrogenation of amorphous silicon to increase the temperature processing window of silicon heterojunction solar cells, *Appl. Phys. Lett.* 109 (2016), 31601, <https://doi.org/10.1063/1.4958831>.
- [41] H. Kampwerth, T. Trupke, J.W. Weber, Y. Augarten, Advanced luminescence based effective series resistance imaging of silicon solar cells, *Appl. Phys. Lett.* 93 (2008), 202102, <https://doi.org/10.1063/1.2982588>.